Science of Sintering, **51** (2019) 199-208

doi:https://doi.org/10.2298/SOS1902199Z

UDK: 546.824; 621.926.087; 622.785

Analysis of the Initial-Stage Sintering of Mechanically Activated $SrTiO_3$

J. Živojinović[1*)], V. P. Pavlović[2], N. J. Labus[1], V. A. Blagojević[1], D. Kosanović[1], V. B. Pavlović[1]

[1]Institute of Technical Sciences of the Serbian Academy of Sciences and Arts, Knez Mihailova 35/IV, 11000 Belgrade, Serbia

[2]University of Belgrade, Faculty of Mechanical Engineering, Kraljice Marije 16, 11120 Belgrade 35, Serbia

Abstract:

The initial-stage of sintering plays a significant role in determining the final microstructure that defines the main characteristics of electroceramics materials such as functional properties. In this article non-isothermal sintering of non-activated and mechanically activated $SrTiO_3$ samples was investigated up to 1300 ^oC. Dilatometric curves indicate that mechanical activation leads to an earlier onset of sintering, suggesting that it should lead to a more homogenous and denser sintered product. Analysis of the initial stage of sintering reveals that the sintering process of all examinated samples consists of two or three overlapping single-step processes, with a change in the dominant mass transport mechanism. The values of apparent activation energy of the considered single-step process exhibit a significant decrease with an increase in mechanical activation time. The values of the density of samples after isothermal sintering indicate that the final stage of sintering has not been reached by 1300 ^oC.

Keywords*: Strontium titanate; Mechanical activation; Dilatometry; Sintering.*

1. Introduction

In the fabrication process of the advanced electroceramics materials, preparation conditions, and especially sintering, are important factors which can significantly affect the mechanical and functional properties of these materials [1, 2]. Strontium-titanate ($SrTiO_3$) is a very attractive functional electroceramic material because of its remarkably high dielectric permittivity, tunability and low microwave loss [3, 4]. The high dielectric constant of $SrTiO_3$ allows its usage in high-storage-density capacitors (dynamic random access memory-DRAM), and various microwave devices [5-7]. These applications require materials with well-defined microstructure: homogeneous micro-grains and low impurity levels [8]. Conventional methods of obtaining $SrTiO_3$ produce large, non-uniform and agglomerated particles with phase impurities, and require high-purity precursors, making them too expensive for industrial production. One of the most used methods for modification of physico-chemical properties of materials is mechanical activation of powders [9], which leads to a reduction of the particle size, increase of the contact surface between particles, plastic deformation of particles, generation of the different type of defects and the formation of soft agglomerates [10-12]. All

*) **Corresponding author:** zivojinovic.jelena@gmail.com

these changes affect the sintering behavior of powders and influence the final properties of the material.

During the sintering process, rapid shrinkage occurs while thermal equilibrium is being established and stresses accompany the rapid heating necessary for isothermal sintering studies [13]. Therefore, the initial part of the sintering process has been studied by measuring densification of the powder compact under the constant rates of heating (CRH). The advantage of this method is that it is fast and a single sample can be used to cover the entire sintering range [14]. CRH method can also be combined with other non-isothermal methods, such as Dorn's method, in order to determine the values of apparent activation energy of sintering processes. A study of the influence of mechanical activation on sintering of materials with perovskite structure has shown that the values of activation energy were lower for activated powders compared to the non-activated one [15]. A study of sintering kinetics of non-stoichiometric $SrTiO_3$, where Sr/Ti ratios ranged from 0.997 to 1.02, indicated that the values of the activation energy for the initial stage of sintering are relatively close to each other for each ratio ($540 \leq Q \leq 674$ kJ/mol) and identical transport mechanisms control the densification process regardless of the sample stoichiometry [16]. The most recent studies of sintering of $SrTiO_3$ have mainly been focused on grain growth in the final stage of sintering [17-19].

Therefore, in this paper we have focused on the influence of mechanical activation on the early stage mechanism of non-isothermal sintering of $SrTiO_3$.

2. Materials and Experimental Procedures

High purity commercial $SrTiO_3$ powder (99 % purity, mean particle size $\leq$ 5 μm) was used as the starting material. Mechanical activation was conducted by ball-milling of 6.5 g of the powder (the powder-to-ball ratio was 1:20) in a 45 cm^3 tungsten carbide jar, in a Planetary micro mill (PULVERISETTE 7 premium line, FRITSCH) for 0, 5, 10, 30, 60, 90 and 120 minutes, in the air. The samples labeled as STO0, STO5, STO10, STO30, STO60, STO90 to STO120, respectively, were pressed into discs of 6 or 8 mm in diameter, under 78.45 MPa. Non-isothermal sintering (d = 6 mm) was carried out in a dilatometer (Bahr Geratebau GmbH802s, Germany) at three heating rates (10, 15 and 20 ^oC/min) in the temperature range from room temperature to 1300 ^oC. The samples were also isothermally treated at 1300 ^oC, for 2 h. Sample density was calculated using the following expression derived from expressions defined in [20, 21]:

$$\rho(t) = \frac{\rho_0}{\left(1-\frac{\Delta L(t)}{L_0}\right)\left(1-\alpha\frac{\Delta L(t)}{L_0}\right)^2}, \quad (1)$$

where L_0 is the initial sample thickness, ρ_0 is the green sample density, $\Delta L(t)$ is the change in sample thickness and α is the anisotropic shrinkage factor. The last one is defined by:

$$\alpha = \frac{(\varphi_f-\varphi_0)L_0}{(L_f-L_0)\varphi_0}, \quad (2)$$

where L_f is the final sample thickness, while φ_f and φ_0 are the final and initial sample diameter, respectively.

Morphology and microstructure of the sintered samples obtained from non-activated and mechanically activated powders were analyzed by a scanning electron microscope (SEM). Measurements were conducted using JSM-6390 LV JEOL (30 kV), where sample tablets were crushed and coated with gold (Au).

3. Results and Discussion

Dilatometric analysis shows that mechanical activation has a prominent influence on the shrinkage during annealing. From Figure 1, which represents the results measured at a constant heating rate of 10 °C/min for four different mechanical activation times (0, 10, 30 and 120 minutes), it can be observed that as the time of mechanical activation increases the temperature corresponding to the onset of shrinkage noticeably decreases.

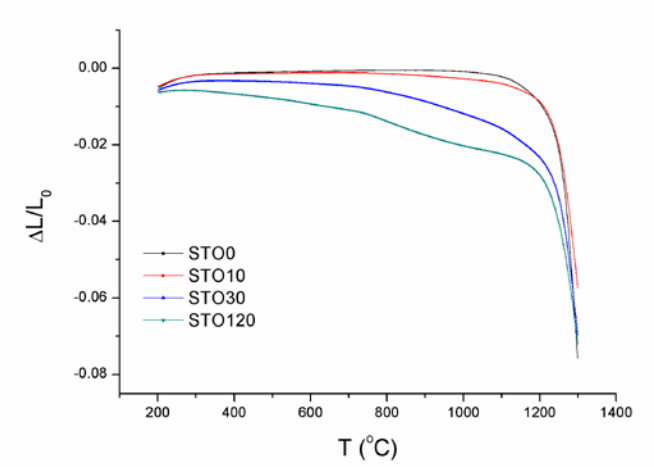

Fig. 1. Relative linear shrinkage as a function of sintering temperature, obtained by dilatometric measurements for STO0, STO10, STO30 and STO120 samples, with a heating rate of 10 °C/min.

The shape of the dilatometric curve and the slopes in different temperature regions change significantly as well, indicating that mechanical activation (especially for 30 min and longer) leads to shortening of the diffusion paths and a more gradual shrinkage within the wider range of annealing temperatures, rather than to a rapid shrinkage process after characteristic sintering temperatures are reached, which was observed for non-activated samples. This suggests that mechanical activation should lead to a more homogenous and denser sintered product.

The influence of activation time on the shrinkage rate during sintering is shown in Figure 2. Since the mechanical activation led to a higher density of pre-sintered pressed powders, i.e. compacts, by 10 to 20 % compared to the non-activated compact, the activated compacts exhibited lower maximal shrinkage rate during the sintering process.

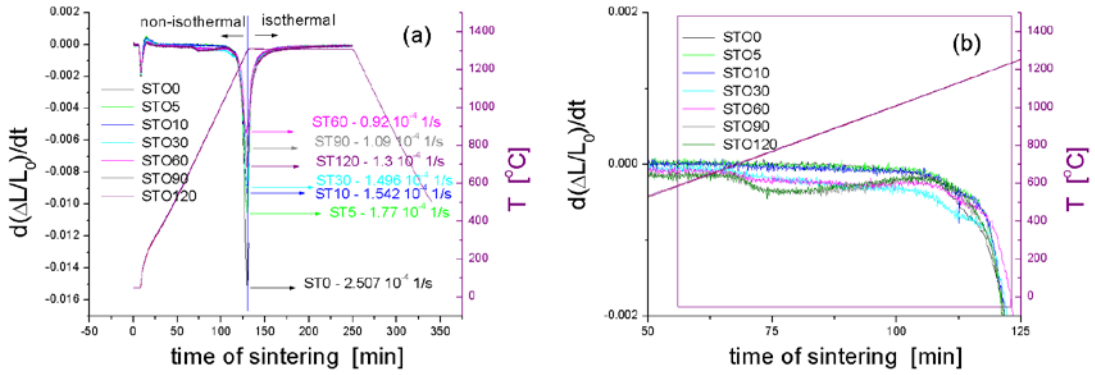

Fig. 2. (a) Shrinkage rate versus time of sintering, with the presentation of the heating profile during sintering. Arrows highlight the positions of maximal shrinkage rate for the samples with different time of activation; (b) Enlarged part of the graph (a).

Figure 2b emphasizes two effects in the temperature region of 600-1000 ^{o}C and 1100-1200 ^{o}C, respectively. This can be attributed to two main processes, which are immanent for the $SrTiO_3$ ceramics: the motion of dislocations which creation is promoted during milling and the formation of vacancies (especially oxygen vacancies) during heating. It should be mentioned that $SrTiO_3$ is prone to the formation of the dislocation defects [22]. Therefore, a decrease in particle size during milling of $SrTiO_3$ powder is accompanied by the formation of different defects where dislocations are probably dominant, since they can be formed more easily. During annealing, dislocations move and the material structure recovers, while, at the same time, a constant increase in the number of vacancies occurs, followed by their migration from sources to sinks. These processes determine the dominant mass transport mechanisms during heating at a constant heating rate, and it is expected that, as the temperature increases, oxygen vacancies become more important kinetic parameter of mass transport. Although the interaction between single dislocation and vacancies in a monocrystal is mainly influenced by the redirecting vacancy path along the dislocation tube, in the polycrystalline system situation is more complex because the concentration of dislocations plays an important role. When dislocations interact with vacancies, they can climb, form partial dislocations, jogs, or annihilate with vacancies [23]. The type of interaction depends on the concentration of dislocations and vacancies and on the energy introduced to the system either by heating or by stress introduction process. Dislocations can glide through the crystal, aggregate - pile up, forming braids and/or low-angle grain boundaries [24]. Since a large number of defects can be induced by milling, it is expected that an annihilation of vacancies and various forms of organized dislocations takes place during heating, as well as the formation of low angle grain boundaries [24].

In Figure 2, the shrinkage rate during annealing in the region from 600 ^{o}C to 800 ^{o}C is higher for the powders mechanically activated for more than 10 minutes, which can be attributed to the movement of dislocations, facilitated occurrence of dislocation climb and their annihilation with vacancies. Lower energy is required for the dislocations mutual interactions [25] in the mechanically activated samples, because the concentration of dislocations is relatively high in these samples at lower temperatures of annealing. With the increase of the concentration of oxygen vacancies, interactions of dislocations with vacancies are more pronounced, evidently influencing the diffusion process [26-28]. Considering the dilatometric effect in the region of 1100-1200 ^{o}C, it can be assumed that additional shrinkage and deviation from the usual behavior at the onset of the sintering shrinkage can originate from the formation of low angle grain boundaries, caused by dislocation pile-up [24] and from the consequential change in the process of oxygen vacancies diffusion. After the non-isothermal annealing, all specimens exhibited the onset of the recrystallization process instantaneously with the change in the heating regime from non-isothermal to isothermal. This is manifested as a sharp peak of the maximal sintering rate, indicating that antagonism of different types of defect recombination provokes relaxation through recrystallization, where recrystallization sites are hard to form and unstable. Since the onset of the isothermal interval brings decrease in the concentration of vacancies and the prompt onset of the recrystallization process, this prohibited the application of the master sintering curve method for determination of the activation energy and led to the application of more conventional methods of calculation of activation energy, by using the initial stage of the sintering process.

Dependence of density on the sintering temperature up to 1300 ^{o}C is shown in Figure 3. The figure confirms that density obtained after non-isothermal regime increases with time of activation.

The density of samples STO0 and STO10 does not change noticeably until the temperature reaches value of around 1100 ^{o}C, while it rapidly increases above 1230 ^{o}C. In the case of samples STO30 and STO120, density begins to gradually increase at lower temperatures (around 750 and 550 ^{o}C, respectively), with a sharp rise above 1200 ^{o}C. The final densities, obtained after non-isothermal annealing up to 1300 ^{o}C and isothermal holding

at this temperature for 2 h, were higher for the STO10 ($\rho \sim 4.08$ g/cm^3) and STO30 ($\rho \sim 4.04$ g/cm^3) samples, compared to the STO120 ($\rho \sim 3.96$ g/cm^3) and STO0 ($\rho \sim 3.59$ g/cm^3) samples.

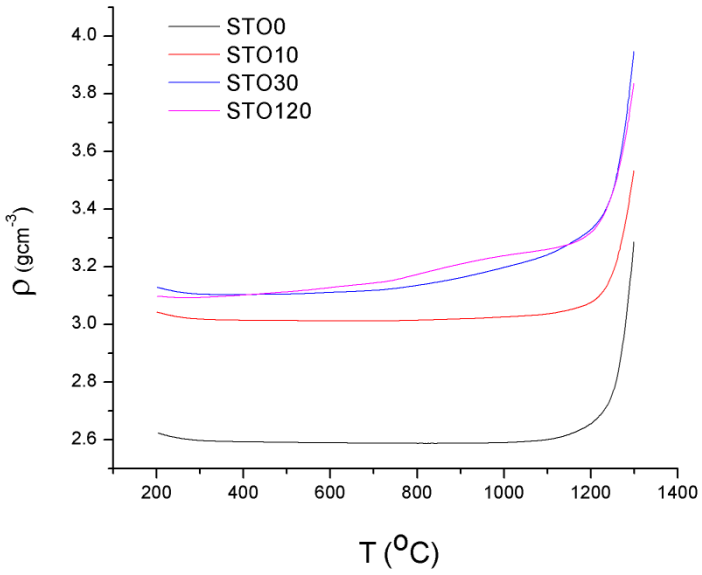

Fig. 3. Dependence of density of STO0, STO10, STO30 and STO120 pressed powders on the temperature during non-isothermal sintering with a heating rate of 10 ^{o}C/min.

Such behavior can be correlated to different types of microstructures observed in the analyzed samples by SEM (Fig. 3) and to different diffusion paths inside and outside of agglomerates. The microstructure of non-activated sample (STO0) contains mainly polyhedral grains with rounded edges and polyhedral grains fused together, with presence of pores, while microstructures of activated samples STO10 and STO30 are denser and less porous (Fig. 3 (a, c, d)). The samples STO10 and STO30 showed higher relative density after the sintering process, although some presence of secondary agglomerates is observed in the STO30 sample. Samples activated for 120 minutes exhibited regions of sintered polyhedral grains and regions of relatively spherical agglomerates (Fig. 3 (g)). The presence of agglomerates can slow down the total densification of the sample and lead to lower values of density during the sintering process [29]. This occurs due to less efficient and postponed inter-agglomerate sintering, compared to the intra-agglomerate sintering, or compared to the densification between densely packed particles that surround an agglomerate. Furthermore, literature suggests that agglomerates may be subjected to compressive stresses, while tensile stresses exist in the surrounding matrix, which inhibits the densification of the green pellet [21].

Samples activated for 5 minutes, compared to the non-activated samples, have a higher density with a slight reduction in pore size and increased fracturing through grain (Fig. 3 (a, b)). Mechanical activation intensifies the transport processes resulting in a less porous microstructure. STO5 sample has a more uniform grain size distribution compared to STO10 sample, while STO10 has more fractures through grain (Fig. 4 (c)). For the activation longer than 30 minutes, enhanced sintering of the grains within the agglomerates was observed (Fig. 3 (d, e)), where agglomerates became significantly more compact, with increased inter-agglomerate porosity. In the samples activated for longer than 60 min spherical pores were not observed, suggesting that the sintering has not entered the final stage (Fig. 3 (f)). In sintered STO120 sample a larger proportion of smaller particles was formed (Fig. 3 (g)).

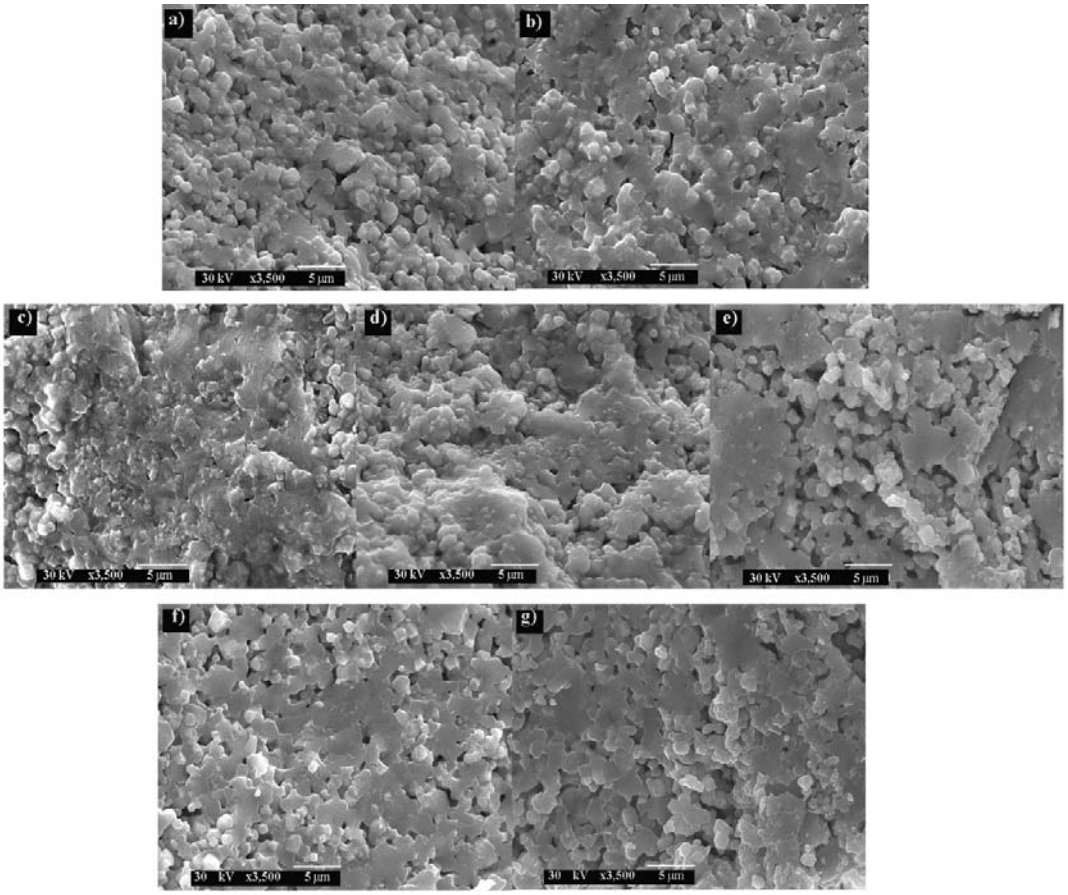

Fig. 4. SEM microstructures of $SrTiO_3$ samples sintered at 1300 °C for 2 h, obtained: (a) from non-activated powders and (b)-(g) from powders activated for 5, 10, 30, 60, 90 and 120 min, respectively.

For the further evaluation of the impact of mechanical activation on the kinetics of early stage of non-isothermal sintering, we applied one of the equations suggested by Woolfrey and Bannister [10], based on the analysis of the shrinkage rate of pressed powder during annealing with a constant rate of heating:

$$T^2 \frac{d\left(\frac{\Delta L}{L_0}\right)}{dt} = \frac{aQ}{(m+1)R}\left(\frac{\Delta L}{L_0}\right), \qquad (3)$$

where T is the temperature in K, a is the rate of heating, Q is the value of the apparent activation energy of the process responsible for shrinkage and sintering, m is a parameter which characterizes dominant mass transport mechanism and R is the gas constant. Figure 5 shows the influence of mechanical activation on the slope of the plot of $T^2 d(\Delta L / L_o)/dt$ vs $(\Delta L / L_o)$ in the early stage of sintering. It was observed that value of $Q/(m+1)$ ratio decreases with the increase in activation time, indicating that value of the apparent activation energy decreases and/or parameter m increases due to applied mechanical activation, which usually may be related to change in the dominant mass transport mechanism. The shape of the curve for each sample implies a complex process of sintering, composed of two or three overlapping single-step processes.

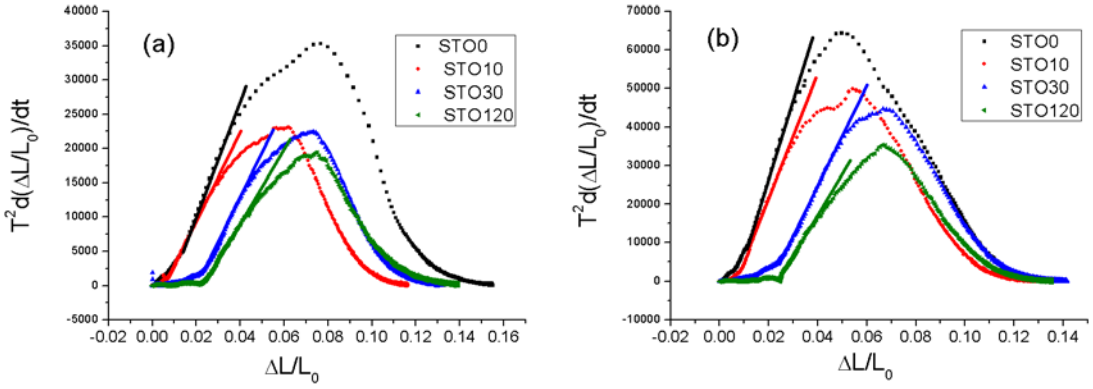

Fig. 5. The plot of $T^2 d(\Delta L / L_o)/dt$ vs $(\Delta L / L_o)$ for a heating rate of (a) 10 °C/min and (b) 20 °C/min.

Dorn's method was used to assess the influence of mechanical activation on the value of the effective apparent activation energy (Q) of the initial stage of sintering. Since the annealing conditions of different STO samples were the same, this provides a relatively reliable assessment of the influence of the mechanical activation. The calculation was performed according to the expression [10, 15]:

$$Q = \frac{RT_1T_2}{T_2 - T_1} ln\left(\frac{v_2}{v_1}\right), \qquad (4)$$

where υ_1 is the shrinkage rate at temperature T_1 (K) and υ_2 is the shrinkage rate at T_2 (K). The results obtained with a heating rate of 10 °C/min show the reduction of the Q value from 720 kJ/mol for the non-activated sample to ~ 520 kJ/mol for STO10 and STO30 samples and to 420 kJ/mol for STO120. The Q value for non-activated sample is close to the values of sintering activation energies of commercial-grade oxide compounds, including perovskite oxides [30]. Since Dorn method had been applied in titanate ceramics with a heating rate as high as 45 °C/min [31], we additionally analyzed the results recorded with 20 °C/min. The Q values obtained from dilatometric measurements with this higher heating rate decreased continuously from the 840 kJ/mol to 650, 510 and 420 kJ/mol, for STO0, STO10, STO30 and STO120 samples respectively, thus confirming the trend of decreasing Q value due to mechanical activation of initial powders. Lower values of the apparent activation energy of sintering process, obtained for the mechanically activated samples, can be correlated with the fact that the linear shrinkage begins at considerably lower temperatures than in the non-activated sample.

4. Conclusion

In this paper, early stage sintering mechanisms of mechanically activated and non-activated $SrTiO_3$ powder were analyzed. It has been noticed that different time-regimes of mechanical activation led to the various combinations of processes of a reduction of particle size and formation of agglomerates, which resulted in different microstructures. It was found that the maximum of the shrinkage rate depended on the density of pre-sintered pressed powders, where the green compacts of activated powders had a higher density compared to the non-activated powder, which led to their faster shrinkage. The higher final densities of samples STO10 and STO30, compared to the STO0 and STO120, were observed after

isothermal sintering, but the values of final density suggested that the sintering has not entered the final stage. Analysis of the shrinkage rate of pressed powders, during annealing with a constant rate of heating, pointed out the complexity of the sintering process consisted of two or three overlapping single-step processes for each sample. The values of apparent activation energies, calculated using Dorn's method, exhibit a significant decrease with an increase in mechanical activation time, with the corresponding shift of the onset of sintering to lower temperatures. These results can be used to further optimize the sintering process of mechanically activated perovskite ceramics.

Acknowledgments

This investigation was supported by the Serbian Ministry of Education, Science and Technological Development, and it was conducted under the OI 172057 project.

5. References

1. H. Naceur, A. Megriche, M. E. Maaoui, "Effect of sintering temperature on microstructure and electrical properties of $Sr_{1-x}(Na_{0.5}Bi_{0.5})_xBi_2Nb_2O_9$ solid solutions", J. Adv. Ceram. 3 (2014) 17-30.
2. V. Paunovic, V. V. Mitic, M. Đordjevic, M. Marjanovic, Lj. Kocic, "Electrical Characteristics of Er-Doped $BaTiO_3$ Ceramics", Sci. Sinter. 49 (2017) 129-137.
3. D. A. Kosanovic, V. A. Blagojevic, N. J. Labus, N. B. Tadic, V. B. Pavlovic, M. M. Ristic, "Effects of Chemical Composition on Microstructural Properties and Sintering Kinetics of (Ba, Sr)TiO_3 Powders", Sci.Sinter. 50, 1 (2018) 29-38.
4. J. Han, F. Wan, Z. Zhu, "Dielectric response of soft mode in ferroelectric $SrTiO_3$", Appl. Phys. Lett. 90 (2007) 031104.
5. A. A. Sirenko, C. Bernhard, A. Golnik, A. M. Clark, J. Hao, W. Si, X. X. Xi, "Soft-mode hardening in $SrTiO_3$ thin films", Nature, 404 (2000) 373-376.
6. P. Kužel, F. Kadlec, H. Nemec, "Dielectric tunability of $SrTiO_3$ thin films in the terahertz range", Appl. Phys. Lett. 88 (2006) 102901.
7. A. K. Tagantsev, V. O. Sherman, K. F. Astafiev, J. Venkatesh, N. Setter, Ferroelectric Materials for Microwave Tunable Applications, J. Electroceram. 11 (2003) 5-56.
8. V. P. Pavlovic, M. V. Nikolic, V. B. Pavlovic, N. Labus, Lj. Zivkovic, B. D. Stojanovic, "Correlation Between Densification Rate and Microstructure Evolution of Mechanically Activated $BaTiO_3$", Ferroelectr. 319 (2005) 75-85.
9. D. L. Zhang, "Processing of Advanced Materials Using High-Energy Mechanical Milling", Prog. Mater. Sci. 49 (2004) 537-560.
10. V. V. Boldyrev, K. Tkacova, "Mechanochemistry of solids: Past, present and future", J. Mat. Synth. And Proc. 8 (2000) 121-132.
11. V. B. Pavlovic, Z. Marinkovic. V. Pavlovic, Z. Nikolic, B. Stojanovic, M. M. Ristic, "Phase Transformations and Thermal Effects of Mechanically Activated $BaCO_3$-TiO_2 System", Ferroelectr. 271 (2002) 391-396.
12. J. Živojinović, V. P. Pavlović, D. Kosanović**,** S. Marković, J. Krstić, V. A. Blagojević, V. B. Pavlović, "The Influence of Mechanical Activation on Structural Evolution of Nanocrystalline $SrTiO_3$ Powders", J. Alloys Compd. 695 (2017) 863-870.
13. W. S. Young, I. B. Cutler, "Initial Sintering with Constant Rates of Heating", J. Am. Ceram. Soc. 53 (1970) 659-663.
14. J. L. Woolfrey, M. J. Bannister, "Non-isothermal Techniques for Studying Initial-Stage Sintering", J. Am. Ceram. Soc. 55 (1972) 390-394.

15. M. V. Nikolic, V. P. Pavlovic, V. B. Pavlovic, M. M. Ristic, "Analysis of Early-Stage Sintering Mechanisms of Mechanically Activated $BaTiO_3$", Sci. Sinter 38 (2006) 239-244.
16. L. Amaral, A. M. R. Senos, P. M. Vilarinho, "Sintering kinetic studies in nonstoichiometric strontium titanate ceramics", Mater. Res. Bull. 44 (2009) 263-270.
17. W. Rheinheimer, M. J. Hoffmann, "Non-Arrhenius behavior of grain growth in strontium-titanate: New evidence for a structural transition of grain boundaries ", Scripta Mater. 101 (2015) 68-71.
18. W. Rheinheimer, M. Baurer, H. Chien, G. S. Rohrer, C. A. Handwerker, J. E. Blendell, M. J. Hoffmann, "The equilibrium crystal shape of strontium titanate and its relationship to the grain boundary plane distribution", Acta Mater. 82 (2015) 32-40.
19. M. Baurer, S. J. Shih, C. Bishop, M. P. Harmer, D. Cockayne, M. J. Hoffmann, "Abnormal grain growth in undoped strontium and barium titanate", Acta Mater. 58 (2010) 290-300.
20. D. Lance, F. Valdivieso, P. Goeuriot, "Correlation between densification rate and microstructural evolution for pure alpha", J. Eur. Ceram. Soc. 24 (2004) 2749-2761.
21. O. Gillia, D. Bouvard, "Phenomenological analysis of densification kinetics during sintering: application to WC-co mixture", Mat. Sci. and Eng. A 279 (2000) 185-191.
22. A. Nakamura, K. Yasufuku, Y. Furushima, K. Toyoura, K.P.D. Lagerlof, K. Matsunaga, "Room-Temperature Plastic Deformation of Strontium Titanate Crystals Grown from Different Chemical Compositions", Crystals, 7 (2017) 351-1-9.
23. P. Hirel, P. Carrez, E. Clouet, P. Cordier, "The electric charge and climb of edge dislocations in perovskite oxides: The case of high-pressure $MgSiO_3$ bridgmanite", Acta Mater. 106 (2016) 313-321.
24. P. Moretti, "Depinning transition of dislocation assemblies: Pileups and low-angle grain boundaries", Phys. Rev. B 69 (2004) 214103.
25. R. Enzinger, Chr. Neubauer, "Kinetics of vacancy annealing upon time-linear heating applied to dilatometry", J. Mater. Sci. 53 (2018) 2758-2765.
26. W. H. Rhodes, W. D. Kingery, "Dislocation Dependence of Cationic Diffusion in $SrTiO_3$", J. Am. Ceram. Soc. 49 (1966) 521-526.
27. M. Broseghini, L. Gelisio, M. D'Incau, C. L. Azanza Ricardo, N. M. Pugno, P. Scardi, "Modeling of the planetary ball-milling process: The case study of ceramic powders", J. Eur. Ceram. Soc. 36 (2016) 2205-2212.
28. D. Marrocchelli, L. Sun, B. Yildiz, "Dislocations in $SrTiO_3$: Easy To Reduce but Not so Fast for Oxygen Transport", J. Am. Chem. Soc. 137 (2015) 4735-4748.
29. H. Ferkel, R. J. Hellmig, "Effect of nanopowder deagglomeration on the densities of nanocrystalline ceramic green bodies and their sintering behavior", Nanostruct. Mater. 11 (1999) 617-622.
30. Science of Sintering: New Directions for Materials Processing and Microstructural Control, edited by H. Palmour III, R.M. Spriggs, D.P. Uskokovic, published in Boston, MA Springer US 1989.
31. Z. S. Macedo, A. C. Hernandes, "A quantitative analysis of the laser sintering of bismuth titanate ceramics", Mater. Lett. 59 (2005) 3456-3461.

Садржај: *Почетни стадијум синтеровања има значајну улогу у дефинисању крајње микроструктуре која утиче на главне карактеристике електрокерамичких материјала као што су то функционална својства. У овом раду је проучено неизотермско синтеровање неактивираног и механички активираних $SrTiO_3$ узорака, у опсегу до 1300 ^oC. Добијене дилатометријске криве указују да механичка активација води ка ранијем почетку процеса синтеровања, што погодује добијању хомогенијих и гушћих синтерованих узорака. Анализа почетног стадијума синтеровања открива да се*

процес синтеровања код свих разматраних узорака састоји од два или три међусобно преклопљена једностепена процеса, при чему долази до смењивања доминантних механизама транспорта масе. При томе, вредности енергије активације датог једностепеног процеса показују значајно смањење са продужавањем времена механичке активације полазног праха. Вредности густина узорака након изотермског синтеровања на 1300 °C сугеришу да финална фаза синтеровања није достигнута ни после изотермског синтеровања.

***Кључне речи**: стронцијум титанат, механичка активација, дилатометрија, синтеровање.*